

# Controlled Amine Functionalization on Conducting Polypyrrole Nanotubes as Effective Transducers for Volatile Acetic Acid

Sungrok Ko and Jyongsik Jang\*

*Hyperstructured Organic Materials Research Center, School of Chemical and Biological Engineering, College of Engineering, Seoul National University, 56-1 Shinlim Kwanak, Seoul 151-742, South Korea*

*Received September 18, 2006*

Pristine (carboxylated) and aminated polypyrrole nanotubes were successfully fabricated using vapor deposition polymerization with a template. In particular, aminated polypyrrole nanotubes were readily synthesized by modifying the nanotube surface with open polyamine chains. Pristine and aminated polymer nanotubes were used as the transducer to acetic acid vapor. Amino-functionalized nanotubes revealed more enhanced sensitivity than the pristine carboxylated nanotubes with the increasing number of amine spacers due to the increased polymer/analyte partition coefficient and mass uptake of the analyte. Moreover, polyamine-functionalized nanotubes presented a reversible and reproducible response to acetic acid up to 40% sensitivity. The aminated polypyrrole nanotubes demonstrated the potential capability to be excellent transducers for volatile fatty acids in disposable sensors.

## Introduction

The accurate and rapid determination of acetic acid concentrations is necessary in industrial food laboratories<sup>1</sup> and disease diagnostics,<sup>2–4</sup> since acetic acid is a component of fermentation products (wines, vinegar, soy sauces, and so on) of which the taste and flavor are affected by the acetic acid concentration. In addition, acetic acid molecules have been focused on in disease diagnostics and used as a biomarker in the breath analysis of patients due to its noninvasive and rapid detection.<sup>5,6</sup> Concentrations of acetic acid were greater in the breath of decompensated cirrhotic patients than in normal subjects. The value of the acetic acid concentration in decompensated cirrhosis was ca. 2730 ppm (670  $\mu\text{g}/100\text{ mL}$  of water condensate breath), while the normal amount for acetic acid was ca. 322 ppm (79  $\mu\text{g}/100\text{ mL}$  of water condensate breath).<sup>7</sup> Therefore, it is very valuable to monitor the concentration of acetic acid vapor in industrial food systems and disease diagnostics.

To date, conducting polymers (CPs) have been extensively investigated for application in chemical sensors, because the conductivity of CPs could be changed by interchain hopping of  $\pi$  electrons.<sup>8–14</sup> The conductivity and physical properties of CPs are influenced by factors such as polaron length and charge transfer to adjacent molecules, which are affected by a specific class of analytes.<sup>15,16</sup> In comparison with their conventional bulk counterparts, CP nanostructures including nanorods, nanofibers, and nanotubes have been of a great interest owing to their high surface area, the amplified sensitivity, and real-time response as a result of enhanced interaction between the conducting polymers and the analytes.<sup>17–19</sup> High contact area between analytes and nanotubes can produce a high density of polaron and bipolaron in conducting polymer main chains, which affect clearly the electrical conductivity of nanotubes. Therefore, the usage of nanotubes as transducers in chemical sensors would result in enhanced and amplified sensitivity. In addition, carboxylated CP nanotubes are one of the excellent candidates for chemiresistive vapor detectors due to abundant surface

functionalities and the relative ease of surface modification. The functionalization of CPs has frequently offered improvements in the selectivity of the resulting chemical sensors. However, there is limited information available concerning the facile surface modification of carboxylated polymeric nanomaterials and their usage as acetic acid sensors. Therefore, it is necessary to develop the tubular functional polymer nanostructures for efficient chemical sensors to specific chemical species as well as observe the distinguished responses of the pristine and surface-modified nanotubes.

Herein, we report the fabrication of open polyamine-modified conducting polypyrrole nanotubes (PPy-NH<sub>2</sub> NTs) and their applications to chemiresistive vapor sensors for acetic acid detection. In particular, carboxylated polymer nanotubes (PPy-COOH NTs) were prepared as the precursor to PPy-NH<sub>2</sub> NTs using vapor deposition polymerization (VDP) mediated with template synthesis. Various amino-functionalized nanotubes were readily synthesized by modifying the nanotube surface with polyamine chains containing a different number of amine spacers. These two different types of nanotubes were used as volatile analyte detectors. Sensitivity and response of functionalized nanotubes were observed as a function of the number of amine spacers and the analyte concentration.

## Experimental Section

**Fabrication of PPy-COOH NTs.** PPy-COOH NTs were prepared by using VDP mediated with template synthesis. Oxidant-impregnated anodic aluminum oxide (AAO) membranes were employed as templates for the nanotubes. To impregnate iron cations into membrane pores, an AAO membrane was soaked in an iron chloride solution (0.1 M) and dried. Subsequently pyrrole-3-carboxylic acid monomer was introduced into the reactor containing an oxidant-impregnated AAO membrane and vaporized for 20 min under  $10^{-2}$  Torr. Polymerization of monomer vapors proceeded at 150 °C for 6 h, and the template was removed with HCl solution (5 M). Consequent PPy-COOH NTs were obtained by washing with ethanol.

**Fabrication of PPy-NH<sub>2</sub> NTs.** PPy-NH<sub>2</sub> NTs were synthesized by functionalizing the surface carboxylates on nanotubes with open

\* Author to whom correspondence should be addressed. Phone: (+82) 2-880-7069. Fax: (+82) 2-888-1604. E-mail: jsjang@plaza.snu.ac.kr.

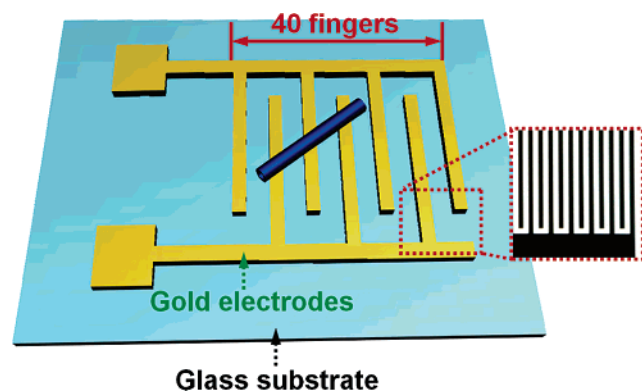


**Figure 1.** Microarray used for measurement of the sensing performance of PPy-COOH NTs and PPy-NH<sub>2</sub> NTs. The magnified photograph is an optical image of gold electrodes.

polyamine chains. Ethylenediamine (EDA), diethylenetriamine (DETA), triethylenetetramine (TETA), and tetraethylenepentamine (TEPA) were employed as open polyamine chain models. Approximately 7 mL of PPy-COOH NTs dispersed in ethanol (0.4 mg mL<sup>-1</sup>) and the excess open polyamines were mixed in 10 mL of ethanol and stirred for 30 min. For a condensation reaction between carboxylic acid moieties of nanotubes and amine moieties of open polyamines, 0.1 g of 4-(4,6-dimethoxy-1,3,5-triazin-2-yl)-4-methylmorpholinium chloride (DMT-MM) was added as a condensing agent. DMT-MM was prepared by reacting 2-chloro-4,6-dimethoxy-1,3,5-triazine and *N*-methylmorpholine in tetrahydrofuran media.<sup>20</sup> DMT-MM was developed for a condensation reaction between a carboxylic acid and a primary amine, which was sterically hindered by a bulky benzene ring. High yields of condensation reactions were found in various substrates and media. In this experiment, surface carboxylic acid would be sterically hindered by polypyrrole main chains. Therefore, DMT-MM was employed to produce a high yield of the surface modification. Final PPy-NH<sub>2</sub> NTs were obtained by washing with ethanol.

**Fabrication of Microelectrodes.** To investigate the sensing performance of nanotubes, a microarray was patterned using a photolithographic process as depicted in Figure 1. The microelectrode device consisted of a pair of gold interdigitated electrodes with 40 fingers (50 nm in thickness on a 50 nm Cr adhesion layer) on a glass substrate. The dimensions of the fingers were 10  $\mu$ m in width, 0.5  $\mu$ m in thickness, and  $4 \times 10^3$   $\mu$ m in length with 10 mm of spacing. PPy-COOH NTs and PPy-NH<sub>2</sub> NTs were deposited by dropping 2  $\mu$ L of the nanotube solution (0.4 mg mL<sup>-1</sup>) on gold electrodes and completely dried in vacuum oven for 30 min. Nanotubes acted as the bridges between disconnected gold leads. The connection of gold electrodes by nanotubes were confirmed by resistance change. The resistance of gold leads was observed by  $6 \times 10^5$   $\Omega$  under PPy-COOH NT connection, while that of disconnected gold leads was above  $2 \times 10^8$   $\Omega$ .

**Resistance Measurement of PPy-COOH NTs and PPy-NH<sub>2</sub> NTs.** The resistances of PPy-COOH NTs and PPy-NH<sub>2</sub> NTs were measured by means of monitoring the potentials at a constant current ( $1 \times 10^{-6}$  A). Nanotube deposition on a gold microelectrode was carried out by dropping 2  $\mu$ L of the nanotube solution dispersed in ethanol (0.4 mg mL<sup>-1</sup>) onto the surface. Completely drying of the electrodes was performed in a vacuum oven for 30 min, and the electrodes were connected to a Keithley 2400 source meter. Resistance was measured at room temperature.

**Sensitivity Measurements of PPy-NH<sub>2</sub> NTs on the Exposure to Acetic Acid Vapor.** The sensitivity of PPy-NH<sub>2</sub> NTs upon exposure to analyte (acetic acid vapor) was defined as the normalized electrical resistance change upon exposure to acetic acid vapor for 60 s and inert nitrogen gas for 180 s. The normalized electrical resistance change was calculated by  $\Delta R/R_0 = (R - R_0)/R_0$ , where  $R$  and  $R_0$  denote the real-time resistance and initial resistance. To investigate the sensitivity of PPy-NH<sub>2</sub> NTs as a function of acetic acid concentration, the sensor substrate was put in a testing chamber equipped with acetic acid and

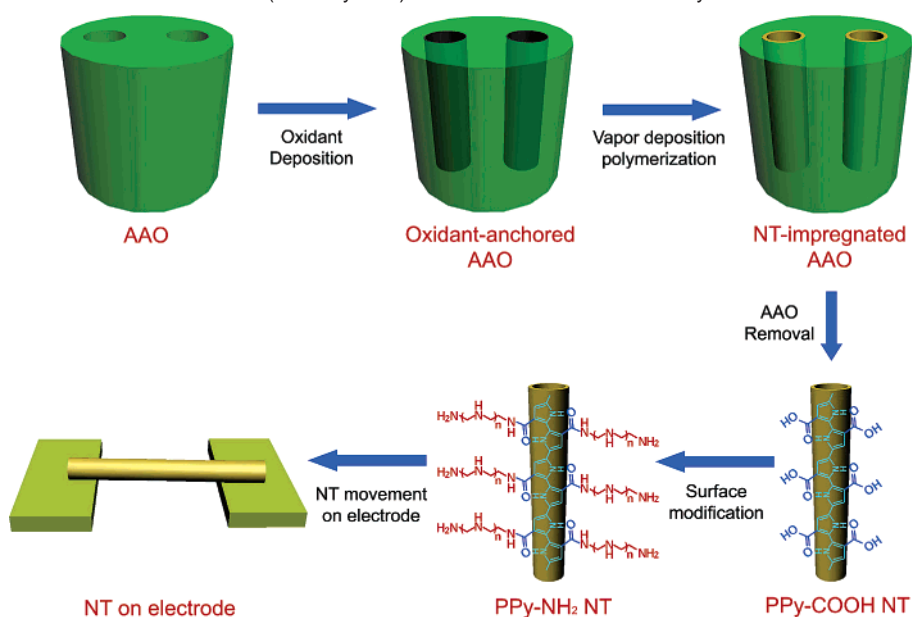
N<sub>2</sub> gas inlets and a waste gas outlet. Initially inert N<sub>2</sub> gas was flowed into the chamber to stabilize the sensor substrates, and the desired concentration of acetic acid vapor was injected by switching the valve. The resistance change of the nanotubes was examined at room temperature in real time with a Keithley 2400 source meter. PPy-NH<sub>2</sub> NTs were periodically exposed to acetic acid and N<sub>2</sub> streams to evaluate the reversibility and reproducibility of the sensors. Exposure to acetic acid and N<sub>2</sub> gas was performed by switching streams with a valve. After acetic acid vapor (230 and 800 ppm) was injected into the chamber, it was replaced by inert N<sub>2</sub> gas. This process was repeated several times. The acetic acid and N<sub>2</sub> streams were supplied at the same flow rate of 2 L min<sup>-1</sup>. The sensitivity was calculated by averaging the normalized resistance of five reversible processes.

**Instrumentation.** Transmission electron microscopy (TEM) images were obtained with a JEOL JEM-200CX. In the sample preparation for TEM, CPPy NTs diluted in ethanol were cast onto copper grids. The acceleration voltage for TEM was 200 kV. Field emission scanning electron microscopy (FE-SEM) was performed with a JEOL 6330F at an acceleration voltage of 10 kV. Raman spectra were recorded on a Horiba Jobin-Yvon TRIAX 550 spectrometer. X-ray photoelectron spectroscopy (XPS) analysis was performed with a Sigma probe Thermo VG under a  $10^{-10}$  Torr high vacuum. Zeta potentials were measured by laser light scattering using a Malvern Zetasizer Nano ZS90. Elemental analysis was conducted with an EA1110 apparatus (CE instruments).

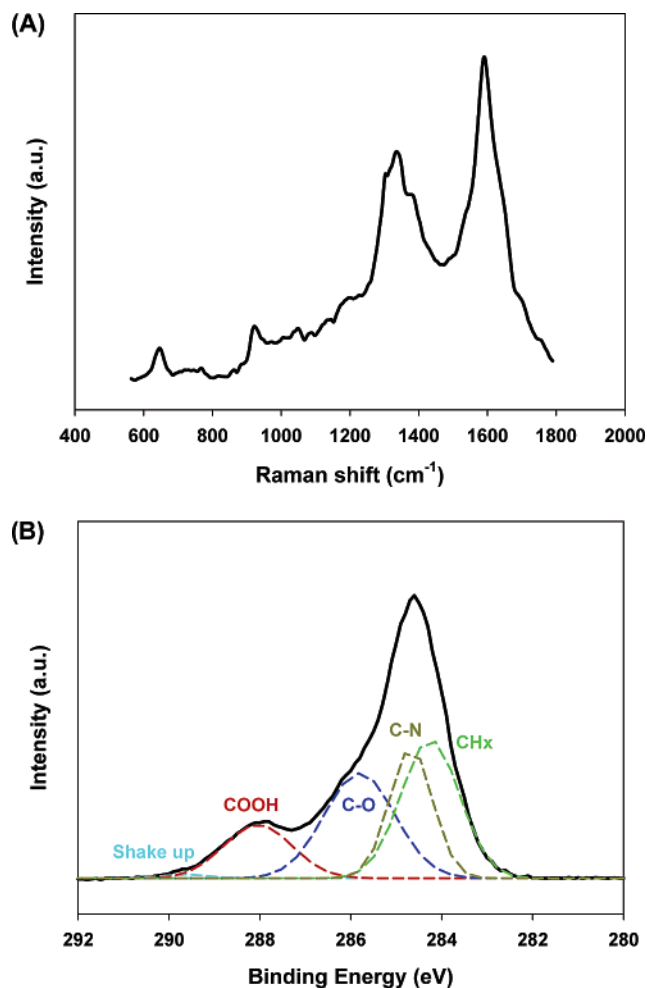
## Results and Discussion

Scheme 1 describes the fabrication of pristine (carboxylated) and amino-functionalized PPy-COOH NTs and the sensing process. PPy-COOH NTs were fabricated using VDP combined with template synthesis.<sup>21–24</sup> Oxidant-impregnated AAO membranes were employed as the nanotube templates, and pyrrole-3-carboxylic acid was polymerized within the AAO pores. Surface modification of the nanotubes was carried out via a condensation reaction. EDA, DETA, TETA, and TEPA were selected as polyamine chain models and applied to PPy-COOH NTs. PPy-NH<sub>2</sub> NTs were readily synthesized by coupling carboxylate moieties of nanotubes with amine groups of polyamine chains. Especially DMT-MM was used as a condensing agent for high product yield.<sup>21</sup> Data for the resistance responses of PPy-COOH NTs and PPy-NH<sub>2</sub> NTs were obtained by exposing the nanotubes on the electrodes at room temperature to increasing partial pressures of the analyte vapor. To initiate an experiment, background nitrogen gas was passed over the chamber containing the nanotube-dispersed electrodes for 10 min. Acetic acid vapor was then passed into the chamber with different concentrations. Resistance was recorded manually using a source meter connected to a computer.

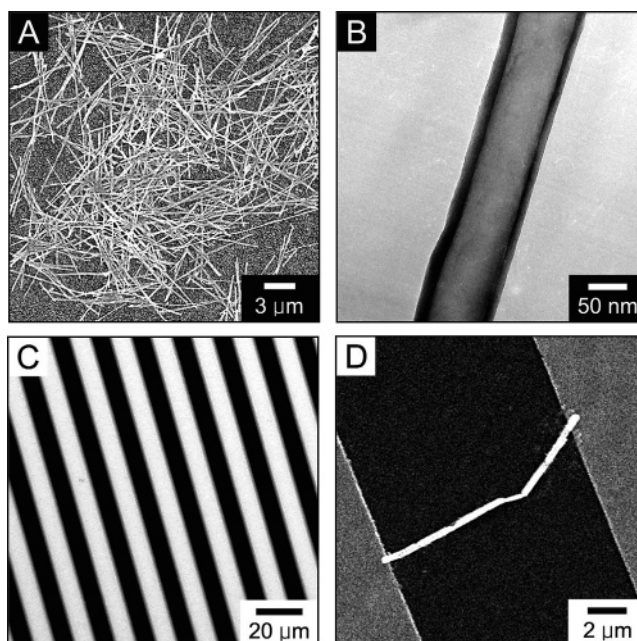
The successful polymerization of pyrrole-3-carboxylic acid monomers was confirmed with Raman and XPS. The characteristic bands of polypyrrole in the Raman spectrum appeared at 927, 1340, and 1592 cm<sup>-1</sup> as the stretching modes of the C-H, C-N, and C=C bands.<sup>25–27</sup> In particular, the peak at 927 cm<sup>-1</sup> was the symmetrical C-H bands in-plane bending assigned as dications (bipolaron). The high intensity of the bipolaron peak at 927 cm<sup>-1</sup> presented the high charge carrier density, which was related to the high electrical conductivity.<sup>25</sup> The peak intensity ratio (0.93) of C-H in-plane deformation at 1053–1091 cm<sup>-1</sup> further demonstrated the relatively high conjugation length and the high conductivity of PPy-COOH NTs.<sup>26</sup> In fact, the conductivity of PPy-COOH NTs was  $2.5 \times 10^{-2}$  S cm<sup>-1</sup> in spite of the presence of carboxylate functional groups in the polymer backbone. The shoulder peak at 1702 cm<sup>-1</sup> also described the presence of carbonyl groups in the

**Scheme 1.** Diagram of the Fabrication of Pristine (Carboxylated) and Amino-Functionalized PPy-COOH NTs and the Sensing Process<sup>a</sup>

<sup>a</sup> EDA, DETA, TETA, and TEPA are represented by  $n = 0, 1, 2$ , and  $3$ , respectively.

**Figure 2.** (A) Raman spectrum of PPy-COOH NTs and (B) XPS spectrum relevant to C<sub>1s</sub> of PPy-COOH NTs.

polymer backbone.<sup>27</sup> Figure 2B depicts the XPS spectrum relevant to C<sub>1s</sub> of PPy-COOH NTs. The peak at 288.2 eV shows the clear existence of carboxylic acid groups in polymer nanotubes.<sup>28</sup> C<sub>1s</sub> peaks were fitted with four curves, and the respective curves were attributed to CH<sub>x</sub>, C-N, C-O, and

**Figure 3.** (A) FE-SEM and (B) TEM images of PPy-COOH NTs, (C) OM image of the electrode, and (D) FE-SEM image of PPy-COOH NTs bridging two gold electrodes.

COOH from 284.8 to 288.2 eV.<sup>29</sup> These results were consistent with the previous carboxylated polypyrrole latex and shifted toward the low binding energy by ca. 1.5 eV. A  $\pi-\pi^*$  shake-up peak at 290 eV appeared as a characteristic of aromatic carbon species.

Figure 3 shows FE-SEM and TEM images of PPy-COOH NTs and an optical microscopy (OM) image of the electrode. VDP combined with template synthesis generated the tailored carboxylated polypyrrole nanotubes, which had a high aspect ratio of greater than 100, a diameter of 100 nm, and a wall thickness of 10–15 nm. In Figure 3A, the FE-SEM image exhibits abundant and uniform PPy-COOH NTs. The lengths of the nanotubes were up to 20  $\mu\text{m}$ . The TEM image in Figure 3B depicts that the tubular structure of the carboxylated polymer nanotube could be clearly observed. These inner vacant spaces



**Table 1.** Elemental Analysis of Pristine (Carboxylated) and Surface-Modified PPy-COOH NTs

NT type	polyamine	element (mol %)		N/C ratio
		C	N	
PPy-COOH NT		2.54	0.57	0.22
PPy-EDA NT	<chem>NCCN</chem>	2.63	0.92	0.35
PPy-DETA NT	<chem>NCCNCCN</chem>	2.75	1.02	0.37
PPy-TETA NT	<chem>NCCNCCNCCN</chem>	2.82	1.07	0.38
PPy-TEPA NT	<chem>NCCNCCNCCNCCN</chem>	2.91	1.16	0.40

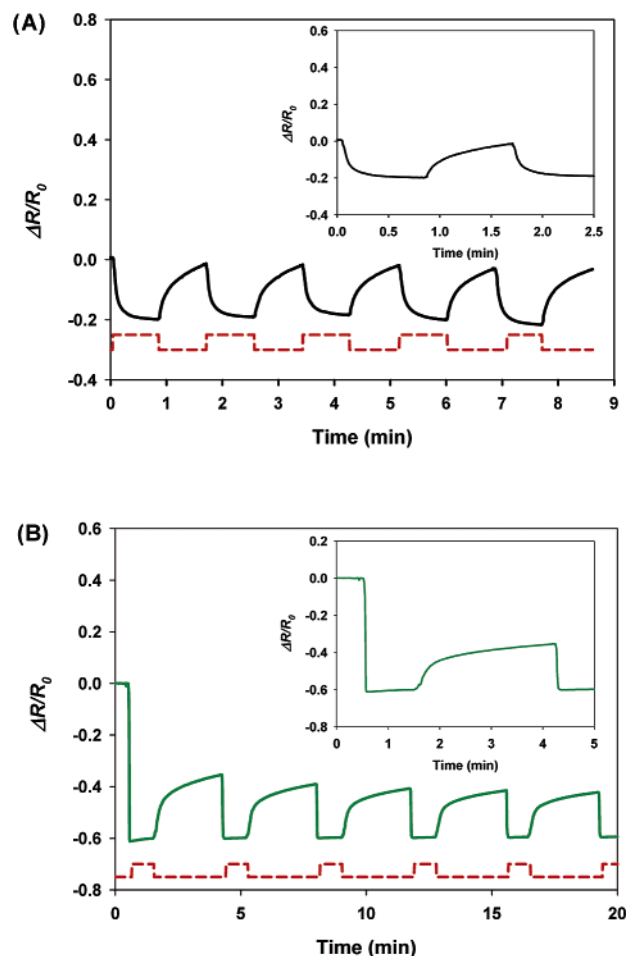
**Table 2.** Zeta Potential of PPy-COOH NTs and PPy-NH<sub>2</sub> NTs

NT type	zeta potential (mV)
PPy-COOH NT	-30.0
PPy-EDA NT	+21.1
PPy-DETA NT	+22.5
PPy-TETA NT	+24.3
PPy-TEPA NT	+25.8

and different outer surfaces were typical characteristics of the nanotubes. Figure 3C presents the features of the gold electrodes using OM. The electrodes were composed of 80 gold leads of 10  $\mu\text{m}$  in width and 10  $\mu\text{m}$  in spacing. This dimension was appropriate to measure the resistance of PPy-COOH NTs. Figure 3D illustrates a FE-SEM image of PPy-COOH NT bridging the two gold leads. Successful connection between two gold electrodes was clearly visualized. Approximately 65 successfully connected nanotubes between electrodes were counted by a drop of 2  $\mu\text{L}$  of PPy-COOH NTs (0.4 mg mL<sup>-1</sup>). These results indicated that PPy-COOH NTs could be excellent materials as electrochemical transducers for chemical detection owing to well-defined morphology. Conductance changes were monitored by resistance measurements of PPy-COOH NTs at a constant current of  $1 \times 10^{-6}$  A.

Table 1 summarizes the elemental analysis data of pristine and surface-modified PPy-COOH NTs. Carbon and nitrogen were chosen, and the molar ratio of nitrogen to carbon was investigated for confirmation of the successful surface modification of nanotubes. The theoretical N/C molar ratio of pristine PPy-COOH NTs was 0.2. In this experiment, the N/C ratio was found to be 0.22 similarly. However, surface-modified nanotubes showed a higher ratio of N/C owing to the abundant nitrogen of open polyamine chains. As the number of amine spacers ( $\text{H}_2\text{C}-\text{HN}-\text{CH}_2$ ) increased, the molar ratio of nitrogen to carbon gradually increased. Judging from these data, it could be thought that the nanotube surfaces were clearly functionalized with polyamine chains.

In addition, the surface characteristics of PPy-COOH NTs and PPy-NH<sub>2</sub> NTs were examined by zeta potential. To measure the zeta potentials of nanotubes, 0.1 wt % of each nanotube solutions were prepared. Carboxylated and aminated polymer nanotubes were dispersed in distilled water and inserted in the folded capillary cells. The zeta potentials were measured using a laser light scattering method with a Malvern Zetasizer Nano ZS90, and their zeta potentials are summarized in Table 2. The zeta potential of modified PPy-NH<sub>2</sub> NTs ranged from +21.1 to +28.8 mV, while that of pristine PPy-COOH NTs was -30 mV at room temperature. As the nanotubes were functionalized with polyamine chains, the zeta potential moved toward the positive direction, because the negatively charged nanotube surface was converted to positively charged amine

**Figure 4.** Exposure of (A) PPy-COOH NTs and (B) PPy-EDA NTs to acetic acid vapor (800 ppm). Nitrogen gas was passed over the detectors for 60 and 180 s, respectively. Each total flow rate was fixed at 2 L min<sup>-1</sup>. Red dotted lines are the periodic input signal of the analyte. The insets are the magnified responses of PPy-COOH NTs and PPy-EDA NTs, respectively.

groups. These pristine and modified CP nanotubes would be appropriate to monitor the influence of surface functional groups on a chemiresistive detector for volatile fatty acids. The resistances of PPy-COOH NTs and PPy-NH<sub>2</sub> NTs were measured by means of monitoring the potentials at a constant current ( $1 \times 10^{-6}$  A). Nanotube deposition on a gold micro-electrode was carried out by dropping 2  $\mu\text{L}$  of nanotube solution (0.4 mg mL<sup>-1</sup>) onto the surface. A completely dried electrode was connected with a Keithley 2400 source meter, and resistance was measured at room temperature. The resistances of PPy-NH<sub>2</sub> NTs ranged from  $7 \times 10^6$  to  $5 \times 10^7$   $\Omega$ , while that of PPy-COOH NTs was  $6 \times 10^5$   $\Omega$ . As the number of amine spacers ( $\text{H}_2\text{C}-\text{HN}-\text{CH}_2$ ) increased, the resistance of PPy-NH<sub>2</sub> NTs increased due to the role of polyamine chains as insulating materials.

Figure 4 presents the responses of PPy-COOH NTs and EDA-functionalized PPy-COOH NTs (PPy-EDA NTs) upon exposure to acetic acid vapor (800 ppm). To evaluate the sensor performance of nanotubes, the normalized resistance change was recorded and calculated by the following equation

$$\Delta R/R_0 = (R - R_0)/R_0$$

where  $R$  and  $R_0$  denote the real-time resistance and the initial resistance of the nanotubes, respectively. To investigate the

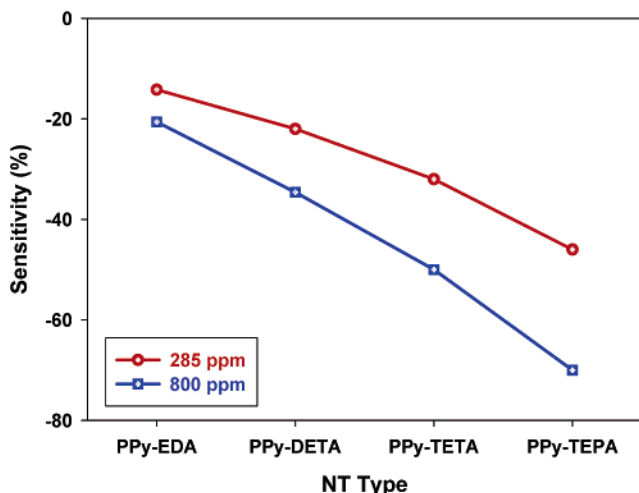


**Figure 5.** Responses of PPY-NH<sub>2</sub> NTs to acetic acid vapor at 285 and 800 ppm.

applicability of PPY-COOH NTs and PPY-NH<sub>2</sub> NTs, those nanotubes were exposed periodically to acetic acid vapor. In Figure 4A, PPY-COOH NTs revealed a gradual decrease in resistance with the exposure to acetic acid vapor and relatively rapid recovery to nitrogen background gas. This phenomenon suggested that acetic acid molecules diffused slowly into the PPY-COOH NTs and the conducting polymer was doped through interaction with acetic acid molecules.<sup>30,31</sup> Negatively charged counter ions (CH<sub>3</sub>COO<sup>-</sup>) were incorporated into the polymer to compensate for the positive charges on the polymer backbone, and the emergence of polarons or bipolarons gave rise to the enhancement in conductivity. In contrast to the behavior of the PPY-COOH NT sensor, PPY-EDA NTs displayed rapid sorption of the analyte and retarded recovery. The faster response time of PPY-EDA NTs than that of PPY-COOH NTs resulted from the enhanced polymer/gas partition coefficient, which was the ratio of the concentration of the vapor molecules in the sorbent phase to the concentration of the vapor molecules in the gas phase.<sup>32,33</sup> It induced a larger mass uptake of acetic acid of PPY-NH<sub>2</sub> NTs than that of PPY-COOH NTs. In addition, the reversible and reproducible responses of PPY-EDA NTs upon analyte exposure indicated that the aminated polymer nanotubes would be good disposable sensor materials for acetic acids. In comparison with inorganic nanomaterials, these conducting polymer nanotubes revealed reversible responses to acetic acid vapors even at room temperature.

Figure 5 demonstrates the sensitivity (defined as the normalized resistance change measured after a 60 s vapor exposure) of PPY-NH<sub>2</sub> NTs functionalized with various polyamine chains to acetic acid vapor. The sensitivity of PPY-NH<sub>2</sub> NTs was measured at both 285 and 800 ppm of acetic acid vapor. Recovery time was restricted to 180 s, because dissociation of acetic acid from nanotubes to recover and reach an initial level took a long time at room temperature. Two different concentrations of acetic acid were selected as the breath models for normal subjects and patients suffering from liver cirrhosis, respectively. The aminated nanotubes revealed increased sensitivity with increasing analyte concentration, since vapor diffusivity was strongly dependent on the analyte concentration. Quite different sensitivity between 285 and 800 ppm indicated the potential applicability of PPY-NH<sub>2</sub> NTs as volatile acetic acid sensors. Moreover, the sensitivity of PPY-NH<sub>2</sub> NTs at 800 ppm increased up to 70%, as the number of amine spacers increased. It originated from the higher polymer/analyte partition coefficient in PPY-NH<sub>2</sub> NTs for enhanced sensitivity at high

concentrations of acetic acid. The significant change of the partition coefficient in PPY-NH<sub>2</sub> NTs would improve the mass uptake of acetic acid and the electrical conductance of nanotubes with an increasing number of amine spacers in the polyamine chains. From the view point of reproducibility, however, PPY-NH<sub>2</sub> NTs functionalized with EDA and DETA were more stable and reproducible for acetic acid analyte than the others. It resulted from the significant polymer swelling caused by periodic mass uptake.<sup>33</sup> Nevertheless, aminated polymer nanotubes showed enhanced sensitivity with increasing numbers of amine spacers. From these results, PPY-NH<sub>2</sub> NTs displayed the potential capability to be volatile acetic acid sensors for disease diagnostics.

## Conclusion

Pristine (carboxylated) and aminated polypyrrole nanotubes were successfully fabricated using VDP with a template followed by surface modification. In particular, aminated polypyrrole nanotubes were readily synthesized by modifying the nanotube surface with open polyamine chains. Both pristine and aminated polymer nanotubes were applied to the transducer for an acetic acid sensor. However, amino-functionalized nanotubes revealed more enhanced sensitivity than the pristine nanotubes due to the increased polymer/analyte partition coefficient and mass uptake of analyte. Moreover, polyamine-functionalized nanotubes presented a reversible and reproducible response to acetic acid up to 40% sensitivity. The aminated polypyrrole nanotubes could be an excellent transducer for volatile acetic acids in disposable sensors.

## References and Notes

- (1) Mizutani, F.; Sawaguchi, T.; Sato, Y.; Yabuki, S.; Iijima, S. *Anal. Chem.* **2001**, *73*, 5738.
- (2) Tillman, E. S.; Koscho, M. E.; Grubbs, R. H.; Lewis, N. S. *Anal. Chem.* **2003**, *75*, 1748.
- (3) Ellis, D. L.; Zakin, M. R.; Bernstein, L. S.; Rubner, M. F. *Anal. Chem.* **1996**, *68*, 817.
- (4) Gao, T.; Tillman, E. S.; Lewis, N. S. *Chem. Mater.* **2005**, *17*, 2904.
- (5) Manolis, A. *Clin. Chem.* **1983**, *29*, 5.
- (6) Phillips, M.; Herrera, J.; Krishnan, S.; Zain, M.; Greenberg, J.; Cataneo, R. N. *J. Chromatogr., B* **1999**, *75*, 729.
- (7) Chen, S.; Mahadevan, V.; Zieve, L. *J. Lab. Clin. Med.* **1970**, *75*, 622.
- (8) Lee, J.-W.; Serna, F.; Nickels, J. Schmidt, C. E. *Biomacromolecules* **2006**, *7*, 1692.
- (9) Swager, T. M. *Acc. Chem. Res.* **1998**, *31*, 201.
- (10) Wang, Y.; Sotzing, G. A.; Weiss, R. A. *Chem. Mater.* **2003**, *15*, 375.
- (11) Korri-Youssoufi, H.; Yassar, A. *Biomacromolecules* **2001**, *2*, 58.
- (12) Hosono, K.; Matsubara, I.; Murayama, N.; Shin, W.; Izu, N. *Chem. Mater.* **2005**, *17*, 349.
- (13) Zhang, X.; Zhang, J.; Song, W.; Liu, Z. *J. Phys. Chem. B* **2006**, *110*, 1158.
- (14) Beattie, D.; Wong, K. H.; Williams, C.; Poole-Warren, L. A.; Davis, T. P.; Barner-Kowollik, C.; Stenzel, M. H. *Biomacromolecules* **2006**, *7*, 1072.
- (15) Jang, J. *Adv. Polym. Sci.* **2006**, *199*, 189.
- (16) Yoon, H.; Chang, M.; Jang, J. *J. Phys. Chem. B* **2006**, *110*, 14074.
- (17) Jang, J.; Chang, M.; Yoon, H. *Adv. Mater.* **2005**, *17*, 1616.
- (18) Jang, J.; Yoon, H. *Langmuir* **2005**, *21*, 11484.
- (19) Jang, J.; Oh, J. H.; Stucky, G. D. *Angew. Chem., Int. Ed.* **2002**, *41*, 4016.
- (20) Kunishima, M.; Kawachi, C.; Iwasaki, F.; Terao, K.; Tani, S. *Tetrahedron Lett.* **1999**, *40*, 5327.
- (21) Jang, J.; Ko, S.; Kim, Y. *Adv. Funct. Mater.* **2006**, *16*, 754.
- (22) Lellouche, J.-P.; Govindaraji, S.; Jeseph, A.; Jang, J.; Lee, K. J. *Chem. Commun.* **2005**, 4357.

- (23) Jang, J.; Oh, J. H. *Chem. Commun.* **2004**, 882.
- (24) Jang, J.; Lim, B. *Angew. Chem. Int. Ed.* **2003**, 42, 5600.
- (25) Liu, Y.-C. *J. Electroanal. Chem.* **2004**, 571, 255.
- (26) Liu, Y.-C.; Hwang, B.-J. *Synth. Met.* **2000**, 113, 203.
- (27) Schmidt, P.; Dybal, J.; Rodriguez-Cabello, J. C.; Reboto, V. *Biomacromolecules* **2005**, 6, 697.
- (28) McCarthy, G. P.; Armes, S. P.; Greaves, S. J.; Watts, J. F. *Langmuir* **1997**, 13, 3686.
- (29) Pope, M. R.; Armes, S. P.; Tarcha, P. J. *Bioconjugate Chem.* **1996**, 7, 436.
- (30) Liu, J.; Lin, Y.; Liang, L.; Voigt, J. A.; Huber, D. L.; Tian, Z. R.; Coker, E.; McKenzie, B.; McDermott, M. J. *Chem.—Eur. J.* **2003**, 9, 604.
- (31) Virji, S.; Huang, J.; Kaner, R. B.; Weiller, B. H. *Nano Lett.* **2004**, 4, 491.
- (32) Grate, J. W.; Kaganove, S. N.; Bhethanabotla, V. R. *Anal. Chem.* **1998**, 70, 199.
- (33) Tillman, E. S.; Lewis, N. S. *Sens. Actuators, B* **2003**, 96, 329.

BM0608885